ISSN 1070-3632, Russian Journal of General Chemistry, 2008, Vol. 78, No. 4, pp. 822–832. © Pleiades Publishing, Ltd., 2008.
Original Russian Text © Yu.A. Ustynyuk, Yu.V. Babin, 2007, published in Rossiiskii Khimicheskii Zhurnal, 2007, Vol. 51, No. 5, pp. 130–138.

Tautomerism of Hydrophosphoryl Compounds and Their Features as Ligands in Metal Complex Catalysis. Quantum-Chemical Simulations by the Density Functional Method

Yu. A. Ustynyuk[a] and Yu. V. Babin[b]

[a]*Chemical Department, Lomonosov Moscow State University, Leninskie Gory 1, build. 3, GSP-2 Moscow, 119992 Russia*
e-mail: ustynyuk@nmr.chem.msu.su

[b]*Pacific State Economical University, Okeanskii pr. 19, Vladivostok, 690091 Russia*
e-mail: buv@list.ru

Abstract—The density functional method (gradient-corrected nonempirical functional PBE, basis TZ2p) was used to perform a large-scale study of the mechanism of tautomerization of hydrophosphoryl compounds RR'P(H)O $\rightleftarrows$ RR'POH (R,R' =Alk, Ar, OR, NR_2). It was shown that intramolecular proton transfer in this rearrangement is forbidden (activation barriers 43.3–60 kcal mol^{-1}), and, in the absence of carrier molecules, it occurs as synchronous transfer of two protons in fairly strong dimeric associates (2.50–10.5 kcal mol^{-1}) formed due to O–H···O, O–H···P, and C–H···O hydrogen bonding. The process involves six-membered transition states with activation barriers of 5–15 kcal mol^{-1}. The contribution of tunneling into the rate constants at 300–400 K, according to estimates in terms of the reaction-path Hamiltonian formalism, reaches 20–40% and increases as the temperature decreases. The mechanism of ethylene hydroformylation in a model complex of a hydrophospohryl compound with Pt(II) [$(H_2PO)_2H$]Pt(PH_3)(H)] was considered to reveal factors responsible for the high efficiency of such complexes in the reaction studied. It was found that the key stages of the catalytic cycle involve reversible proton migration in the –$PH_2OH\cdots O$=P chain of the quasi-chelate ring, which provides fine tuning of the electron distribution in the catalytic node and thus functions as a molecular switcher.

DOI: 10.1134/S1070363208040415

INTRODUCTION

Outstanding recent advances in quantum chemistry in combination with impetuous progress of computational techniques have made quantum-chemical calculations one of the most powerful and low-cost tool of chemical research. Over the past 10–15 years, the most impressive results are associated with the use of high-level quantum-chemical calculations for studying the structure of transition metal complexes and the mechanisms of their catalyzed reactions in solutions [1, 2]. The development and fast introduction of metal complex catalysis techniques in practice has become one the most spectacular achievements of chemical science over the past half-century, which has exerted a revolutionizing influence on laboratory and industrial organic and organometallic synthesis.

The activation of a low-reactivity substrate in a metal complex–catalyzed process is effected via incorporation of the substrate into the coordination sphere of the transition metal. Therewith, complexes of electron-deficient, "early" transition metals (Ti, Zr, V), that exhibit Lewis acid properties, activate substrates with respect to nucleophilic reagents. By contrast, complexes of electron-excessive, "late" transition metals enhance the reactivity of substrates with respect to electrophiles. Tempting perspectives are associated with push–pull activation on simultaneous substrate coordination with two transition metals of different nature ("late–early" metal couple), immediately adjacent to each other in the complex. Even though stoichiometric reactions occurring along this scheme have been reported about [3–6], it has not yet been experimentally realized in the catalytic regime.

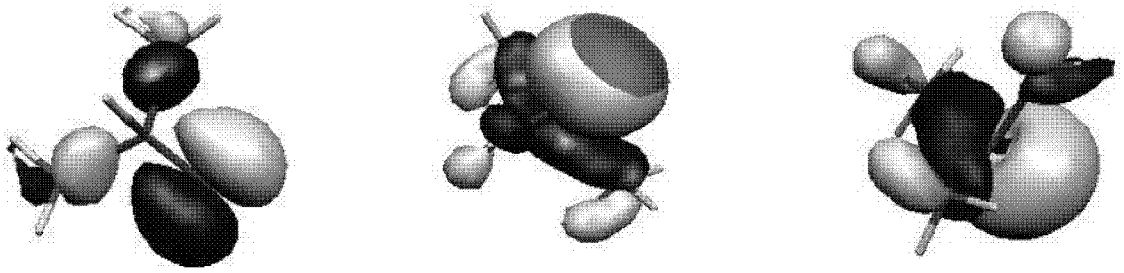

$(CH_3)_2P(O)$ (**VI**) *cis*-$(CH_3)_2POH$ (**VIIa**) *trans*-$(CH_3)_2POH$ (**VIIb**)

Fig. 1. Structure of the highest molecular orbitals of dimethylphosphine oxide **VI** and phosphinous acid **VIIa, VIIb.**

As a rule, the formation of new C–C and C–X bonds in metal complex–catalyzed reactions which has become a major tool for creating new carbon–carbon and carbon–heteroatom bonds over the past decade occurs in the coordination sphere of the metal via inner-sphere rearrangement. Therewith, ligand environment plays an exceptionally important role. By varying donor properties of ligands and also by varying geometry of ligands via using bi- and tridentate ligands or via introducing sterically hindering groups one can profoundly affect the rate and regio- and stereoselectivity of reactions. The use of chiral ligands has opened up the way to enantioselective syntheses for preparing target enantiomers of a very high purity.

The most common mono- and bidentate ligands used in complexes of late transition metals are tertiary phosphines. However, though quite diverse, they have one common disadvantage, viz. quite low resistance to oxidation. For this reason, reactions have to be performed in air-proof conditions with high-purity starting materials, and with large ligand-to-metal rations (up to 100:1). However, even under these precautions, losses of catalysts due to their destruction prove to be quite essential. To enhance the oxidative resistance of phosphine ligands remains one of the most challenging problems of metal complex catalysis. Therefore, the advent of hydrophosphoryl compounds $R_2P(O)H$ as a new type of donor ligands that form oxygen- and moisture-resistant complexes has arose considerable interest.

In the present paper we consider new aspects of the chemistry of hydrophosphoryl compounds and their catalyzed reaction mechanisms in the light of the results of calculation of the structure of these compounds and simulation of reaction mechanisms by the density functional theory (DFT) method. This method has played the key role in the development of the theory of structure and reactivity of complexes and organic derivatives of transition metals, since it provided reliable results for adiabatic potential surfaces of such compounds, containing hundreds light element atoms and a number of higher period element atoms, at fairly modest computational expenses.

Calculation Procedure

Geometry optimization of molecules and transition states was performed by the DFT method with the gradient-corrected functional PBE [7], three-exponential basis set of Gaussian. functions TZ2P [8, 9] for valence electrons, and pseudopotentials SBK-JC [10–12] for core electrons. Steric structures of all the molecular systems studied were fully optimized. Thermodynamic functions were calculated by statistical formulas in terms of the rigid rotor–harmonic oscillator model. Molecular energies in stationary points of the PPE were calculated with zero-point vibration corrections. Intrinsic. reaction coordinate (IRC) calculations were performed for authentication of the revealed transitions states.

All calculations were performed using the PRIRODA program [8, 9]. Frontier orbitals of hydrophosphoryl compounds were calculated using the MOLDEN program [13]. Atomic charges were calculated by Hirshfeld [14].

Tautomerism of Hydrophosphoryl Compounds

Hydrophosphoryl compounds can undergo a tautomeric trasition between two forms: secondary phosphine oxide $R_2P(O)H$ (**I**) and phosphinous acid $R_2P(OH)$ (**II**) which, in its turn, can exist as two rotamers: *trans* (**IIa**) and *cis* (**IIb**). The facile interconversion **I** $\rightleftarrows$ **II** is provided by a unique combination of the properties and reactivities of two

major classes of organophosphorus compounds—P(V) and P(III) derivatives, which makes them quite attractive reagents in organic and organoelement synthesis [15, 16].

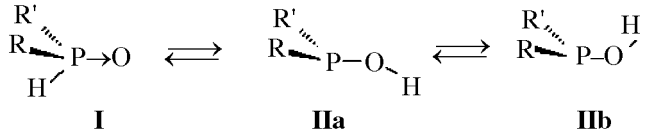

I **IIa** **IIb**

R, R' = alkyl, aryl, alkoxy, aroxy. (1)

If R and R' are donor alkyl and aryl substituents, equilibrium (1) is strongly shifted to oxide **I**. On the contrary, electron-acceptor substituents stabilize the phosphinous acid form.

Among the few hydrophosphoryl compounds present in the tricoordinate form, the best studied is bis (trifluoromethy)phosphinous acid $(CF_3)_2POH$ (**III**) [17, 18]. The tautometic equilibrium between bis (pentafluorophenyl)phosphinous acid (**V**) and bis (pentafluorophenyl)phosphine oxide (**IV**) was established by NMR spectroscopy [17]:

$$\underset{\mathbf{IV}}{(C_6H_5)_2POH} \rightleftarrows \underset{\mathbf{V}}{(C_6H_5)_2POH}. \quad (2)$$

Similar equilibria were detected for ethylene hydrogen phosphite [19] and hydrogen *o*-phenylene phosphite [20]. Our DFT calculations [21, 22] and calculations of other authors [18] nicely reproduce these experimentally revealed tendencies.

Figure 1 shows the HOMO of dimethylphosphine oxide **VI**, as well as dimethylphosphinous acid rotamers **VIIa** and **VIIb**. The HOMO of **VI** is localized on the phosphoryl oxygen, it is degenerate and occupied by two lone electron pairs. The HOMO in phosphinous acids **VIIa, VIIb** is localized on the phosphorus atom and represented by its lone electron pair. This HOMO is mostly contributed by the 3*p*- and 3*s*-AOs of phosphorus, but there is also a minor contribution of the oxygen *p* orbital. Such a HOMO structure give clear evidence showing that phosphinous acids, having the lone electron pair localized on phosphorus, can act as donor ligands with respect to transition metals; this feature distinguishes phosphinous acids from phosphine oxides whose hard donor center is localized on the oxygen atom.

Even though rearrangement (1) in solutions occurs in mild conditions, theoretical calculation show that the activation barriers to intramolecular hydrogen transfer in hydrophosphoryl compounds are quite high [23, 24]. The activation barrier for the model rearrangement of the simplest phosphine oxide $H_2P(O)H$ D H_2POH is 60 kcal mol^{-1} [23] (cc-pVTZ/CCSD(T)). Our DFT calculated activation barriers to intramolecular hydrogen transfer for 20 tautomeric pairs of hydrophosphoryl compounds with different substituents on the phosphorus atom span the range 43.3–52.2 kcal mol^{-1} [21]. This finding makes us to consider alternative intramolecular mechanisms of this rearrangement in solutions, that involve proton carriers. This function can be accomplished by protic solvents, such as water and alcohols. In nonpolar aprotic solvents, the rearrangement should occur as a bimolecular reaction involving at least two hydrophosphoryl compound molecules.

Our calculations showed that hydrophosphoryl compounds form several types of dimers with one and two hydrogen bonds [25]. Thus, *trans*-dimethylphosphinous acid **VIIb** forms quite a strong dimer **VIII** (dimerization energy ΔE_d = –9.07 kcal mol^{-1}) with two O–H···P hydrogen bonds, in which both P–O–H fragments lie in the same plane.

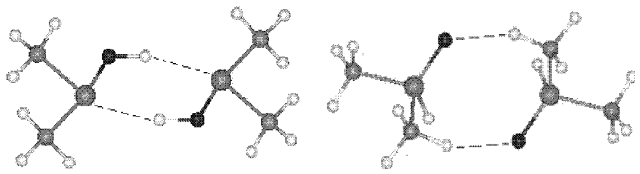

VIII

ΔE_d = –9.07 kcal mol^{-1}

R(P–O) = 1.679 Å

R(P···H) = 2.346 Å

R(O–H) = 0.995 Å

IX

ΔE_d = –6.64 kcal mol^{-1}

R(O···H) = 2.38 Å

R(O···P) = 3.30 Å

By contrast, dimethylphosphine oxide **6** does not form symmetrical diimers with OLH–P hydrogen bonds, since its P–H bond is nonpolar and unable to hydrogen bonding. Nevertheless, we still could identify on the PES a number of local minima corresponding to dimeric associates with acoplanar P(O)H fragments and intermolecular C–H···O hydrogen bonds with methyl hydrogens instead of P–H···O hydrogen bonds. The question of whether and to what measure the relatively weak (1–4 kcal mol^{-1}) C–H···O intramolecular inter-actions can be considered as ordinary hydrogen bond was hotly debated [26–31]. A comprehensive theoretical analysis with use of nonempirical methods showed that such description is quite justified [31].

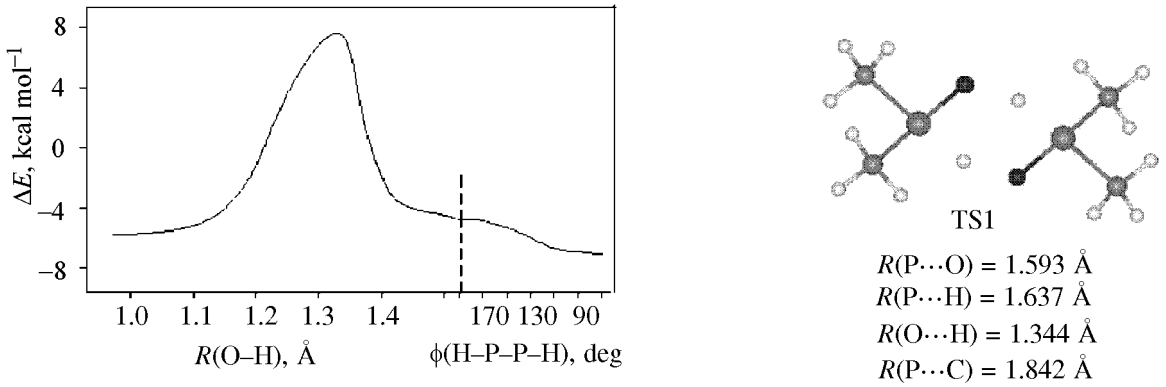

Fig. 2. Reaction coordinate of synchronous transfer of two hydrogen atoms over the course of the rearrangement of dimethylphosphinous acid dimer **VIII** into dimethylphosphine oxide dimer **IX**, and certain characteristics of transition state TS1.

The rearrangement of dimer **VIII**, involving synchronous transfer of both protons in P–O–H···P hydrogen-bond chains [Eq. (3)], leads to dimer **IX** containing two C–H···O hydrogen bonds. Bader's AIM analysis [32] revealed in it two band critical points of the (3, –1) type, corresponding to such hydrogen bonds.

$$(CH_3)_2POH + (CH_3)_2POH \rightleftarrows \mathbf{VIII} \rightleftarrows \mathbf{IX} \rightleftarrows (CH_3)_2P(O)H + (CH_3)_2P(O)H. \quad (3)$$

The rearrangement reaction coordinate has two well-defined branches (Fig. 2). First a symmetrical transition state TS1 is attained via a steady increase of the energy due to the increase of the interatomic distances R(O–H) from 0.995 Å in **VIII** to 1.344 Å in TS1. Along this portion of the reaction path and in the transition state the P–O–H fragments in the dimer remain coplanar. Along the initial portion of the trajectory of descent from TS1 the P–O–H fragments remain coplanar, and the energy steadily decreases until the P···H distances have shortened to 1.431 Å. Therewith, the O···H interatomic distances elongate to 2.453 Å. In this point of the system's Hessian, an imaginary frequency appears, which corresponds to change of the H–P–P–H dihedral angle, and further descent of the potential curve occurs as this angle decreases from 180° to 71° and the P···H distance remains unchanged. The oxide molecules turn with respect to each other about P→O bonds to form two C–H···O hydrogen bonds between phosphoryl oxygens and methyl hydrogens and, eventually, dimer **IX**. The activation barrier in such a bimolecular acid–oxide rearrangement is as low as 4.84 kcal mol^{-1}.

Thus, the tautomeric transitions between phosphinous acid and phosphine oxide in nonpolar media in mild conditions in the absence of proton carriers, experimentally observed in hydrophosphoryl compounds, occur as bimolecular reactions with intermediate formation of dimers via six-membered planar transition states. This mechanism has certain in common with the mechanism of proton migrations in dimers of carboxylic acids, which is essentially tunnel in nature.

One of the simplest and, at the same time, effective tools for studying the chemical dynamics and assessing the tunnel effects in chemical reactions is the reaction path Hamiltonian (RPH) formalism. We made use of the RPH formalism to construct a dynamic model for the simplest phosphinous acid–phosphine oxide rearrangement (4) [33]:

$$H_2P(O)H \rightleftarrows \mathbf{X} \rightleftarrows \mathbf{XI} \rightleftarrows H_2P(O)H. \quad (4)$$

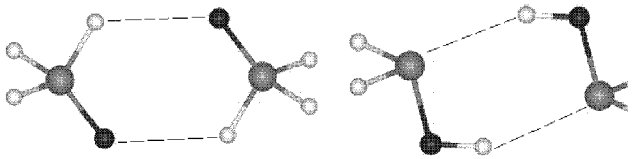

X
ΔE_d = –2.3 kcal mol^{-1}
R(O···H) = 2.411 Å
R(O···P) = 3.369 Å

XI
ΔE_d = –3.2 kcal mol^{-1}
R(P···H) = 2.428 Å
R(O–H) = 0.987 Å

Figure 3 shows the least-energy path potential $V_0(s)$ (dashed line) and variation of the lateral vibration frequencies along the natural reaction coordinate s in Å Å $\sqrt{m_H}$ (m_H is the proton mass, 1847 amu). The left

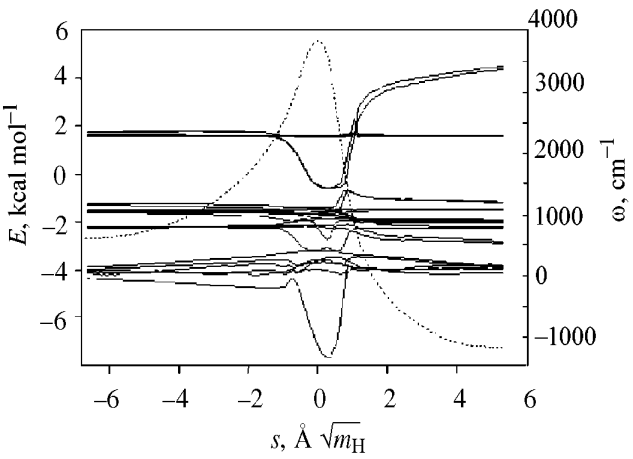

Fig. 3. Least-energy path potential $V_0(s)$ (dashed line) and variation of the lateral vibration frequencies along the reaction coordinate s for rearrangement (4).

minimum corresponds to phosphine oxide dimer **X** and the right, to phosphinous acid dimer **XI**. The system preserves its C_{2h} symmetry along the entire reaction path. Both phosphorus and both oxygen atoms, as well as migrating hydrogen atoms lie in the same plane. The strongest changes along the reaction coordinate are characteristic of the $w_{2,3}(s)$ frequencies which represent symmetric and antisymmetric vibrations q^+(P–H) and q^-(P–H) in the left part of the reaction path and q^+(O–H) and q^-(O–H) of A′ and B′ symmetry, respectively, in the right part. The barrier to forward reaction, corrected for zero-point energy, is 4.1 kcal mol^{-1}.

To assess the contribution of the tunnel rearrangement mechanism, we calculated total rate constants for the forward (k_1^{CUM}) and reverse (k_2^{CUM}) reactions, overbarrier contributions k_1^{ARR} and k_2^{ARR} with overbarrier reflection corrections, as well as trans-mission coefficients c. The tunnel contribution into the total rate constant decreases with decreasing energy. The c coefficient reaches 2 for the forward reaction at $T <$ 165 K and for the reverse reaction, at $T <$ 190 K (at these temperatures, the tunnel and activation contributions get equal to each other), and varies from 1.4 to 1.3 in the temperature range 300–400 K. Thus, the contribution of tunneling into the rearrangement rate is quite large at both room and elevated temperatures.

Complexes of Hydrophosphoryl Compounds with Late Transition Metals

A powerful impetus in the development of the chemistry of hydrophosphoryl compounds has been given by the discovery of Li [34] that the tautomeric equilibrium (1) in the reaction of phosphine oxides with transition metal ions is shifted to phosphinous acids which, like tertiary phosphines, form strong complexes with late transition metals. As shown above, hydrophosphoryl compounds as ligands offer advantage over traditionally used tertiary phosphines in that they and their complexes are much more resistant to oxidation [35]. The principal aspects of the coordination chemistry of hydrophosphoryl compounds are represented in the reviews [36, 37].

In *trans* complexes **XII,** both ligands behave as independent units. Such complexes are readily deprotonated under the action of even weak bases [Eq. (5)], which increases the electron density on the metal atom.

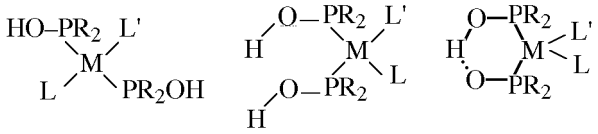

XII **XIII** **XIV**

$$[L_nM(PR_2OH)_2] + B \longrightarrow [L_nM(PR_2O)(PR_2OH)]^- + BH. \quad (5)$$

XV

Therefore, anionic complexes **XV** are much more susceptible to oxidative addition and serve as stable and very active catalysts in various cross-coupling reactions (Kumada–Tamao–Corriu [35], Suzuki–Miyaura [38], Heck, Stiele [39], Sonogashira [40], Negisi [41], etc. [42]), which makes possible to introduce low-reactivity substrates in such reactions.

In *cis*-complexes **XIV,** two inner-sphere phosphinous acid molecules undergo single deprotonation to form a chelating bidenatte monoanionic ligand. Such complexes are quite active and selective catalysts in alkene hydroformylation [43] and alkyne hydrophosphinylation [44]. These compounds are also readily deprotonated under the action of weak bases.

Chiral complexes of hydrophosphoryl compounds on the basis of secondary phosphites with a chiral phosphorus atom were also prepared and studied [45]. Note that the advances in the application of complexes **XII–XIV** in metal complex catalysis proved so impressive that the "CombiPhos" Company [42] launched their commercial production. Complexes in which the oxygen atoms of two hydrophosphoryl compounds (ligands) are bridged by BF_2 and SiR_3 groups or transition metal ions were also synthesized.

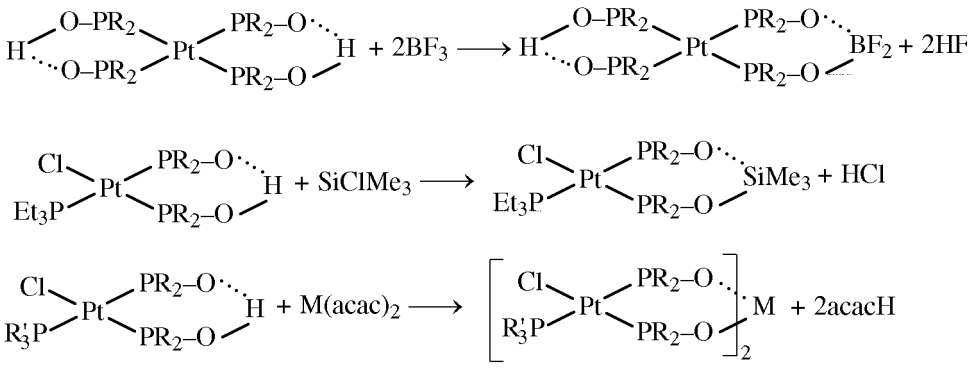

R = OMe, Ph, Et; $M(acac)_2$ = Co or Cu acetylacetonate.

Mechanisms of Hydroformylation and Hydrogenation of Alkenes, Catalyzed by Complexes of Hydrophosphoryl Compounds

Homogeneous hydroformylation of alkenes (oxo synthesis) is the most important method of commercial synthesis of aldehydes:

$$RCH{=}CH_2 + CO + H_2 \rightarrow RCH_2CH_2CHO. \quad (6)$$

Cobalt, rhodium, and palladium complexes are traditionally used as catalysis in such reactions. With cobalt carbonyls, the yields of the target linear aldehydes attain 95%. However, the process involving cobalt carbonyls is disadvantageous in that it requires high temperatures (up to 200°C) and pressures (up to 200 atm) to occur.

A much milder hydroformylation takes place in the presence of rhodium complexes, but here much branched aldehydes are formed. The regioselectivity of the process can be increased by using bidentate ligands [46], but such ligands not infrequenly cost more than the metal itself.

A platinum(II) complex like **XIV** as hydroformylation catalyst was first suggested by Van Leeuwen who showed that the hydroformylation of hept-1-ene on the complex $[(Ph_2PO)_2H]Pt(PPh_3)(H)]$ (**XVI**) occurs in mild conditions with a more than 90% regioselectivity [42]. This complex is formed in solution *in situ* by simply mixing $Pt(cod)_2$ (cod is cycloocta-1,5-diene), PPh_3, and $PPh_2(O)H$. Tanaka et al. [44] prepared similar complexes $[(Ph_2PO)_2H]M(PEt_3)(H)]$ (M = Pt, Pd) by oxidative addition of diphenylphosphine oxide to $M(PEt_3)_3$ and established the structure of platinum complex **XVI** by X-ray diffraction.

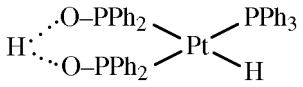

XVII

These authors also showed that the platinum complex actively catalyzes alkylne hydrophosphinylation. Van Leeuwen et al. [43] have traced the hydroformylation of hept-1-enein the presence of **XVI** by accomplishing this reaction in stages under controlled conditions [43]. In the first stage, by passing hept-1-ene into a solution of **XVI** at 25°C they could detect (by NMR) η^1-alkyl complex **XVIII** [Eq. (7)]. Upon subsequent passing of CO this complex converted into complex **XIX** [Eq. (8)] whose reaction with molecular hydrogen gives the final product, octanal [Eq. (9)].

$$\underset{\textbf{XVI}}{L_3Pt{-}H} + C_5H_{11}CH{=}CH_2 \longrightarrow \underset{\textbf{XVIII}}{L_3Pt{-}CH_2CH_2C_5H_{11}}, \quad (7)$$

$$L_3Pt{-}CH_2CH_2C_5H_{11} + CO \longrightarrow \underset{\textbf{IX}}{L_3Pt{-}COCH_2CH_2C_5H_{11}}, \quad (8)$$

$$L_3Pt{-}COCH_2CH_2C_5H_{11} + H_2 \longrightarrow L_3Pt{-}H + C_5H_{11}CH_2CH_2CHO. \quad (9)$$

The fact that complex **XVI** is highly active in the hydroformylation reaction and provides a very good reaction selectivity prompted us to perform a theoretical simulation of the mechanism of this process to find out what factors are responsible for such a combination. The mechanism of hydroformylation was previously studied by different quantum-chemical methods (MP2 [6, 47] and DFT [49, 50]). Both individual stages [6, 48, 49] and complete catalytic cycles [50] were explored. With the $HCo(CO)_4$ catalyst, the limiting stage was elimination of carbon

Geometric parameters of platinum complexes like **XVI**[a]

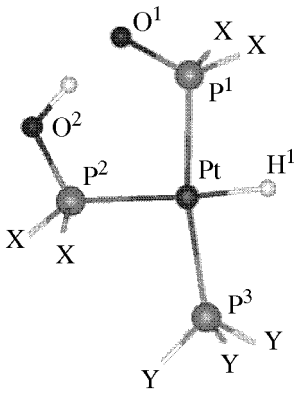

Parameter	**XX**		**XIV**		**XVII** [44]
	X=Y=H	X=Y=Me	X=Ph, Y=Me	X=Y=Ph	X=Ph, Y=Et
$Pt–P^1$	2.315	2.340	2.341	2.334	2.280
$Pt–P^2$	2.353	2.367	2.366	2.378	2.313
$Pt–P^3$	2.323	2.339	2.344	2.372	2.301
$Pt–H^1$	1.633	1.638	1.636	1.630	1.245
$O^1–O^2$	2.470	2.443	2.455	2.462	2.317
$P^1–O^1$	1.563	1.574	1.573	1.569	1.532
$P^2–O^2$	1.607	1.610	1.614	1.617	1.569
$P^1–Pt–P^2$	92.4	92.7	91.6	93.0	92.5
$P^2–Pt–P^3$	98.4	101.8	102.4	107.2	100.7
$P^1–Pt–P^3$	169.2	165.4	165.6	159.8	166.6
$O^1–P^1–Pt$	117.3	116.5	116.8	117.2	114.9
$O^2–P^2–Pt$	117.4	115.5	115.4	114.4	111.4

[a]Bond lengths and interatomic distance are in Å and angles are in deg.

monoxide (first stage), while with $HRh(PR_3)_3(CO)$, insertion of CO into the metal–alkyl σ bond [50].

We performed a detailed theoretical study of the hydroformylation of ethylene in the presence of a model complex $[(H_2PO)_2H]Pt(PH_3)(H)]$ (**XX**) derived from complex **XVI** in which, for lower computational expenses, the aryl groups on phosphorus were replaced by hydrogen.

The calculated geometric parameters of complexes **XVII** and **XX**, together with experimental data for **XVII** [44], are listed in the table. For the sake of comparison, in the same table we give the calculated parameters of a number of structurally similar complexes to illustrate how varying the radical on the phosphorus atom affects the geometry of the coordination entity.

In whole the calculation results fairly fit experiment. The geometry of the coordination entity is a distorted planar square in which the bidentate ligand $[(H_2PO)_2H]^-$ formed by phosphinous acid and its anion is clearly unsymmetrical and has the phosphinous OH hydrogen atom *trans* to the hydride hydrogen. The ligand–metal coordination bond is elongated. The bond lengths and angles are fairly reproduced by calculations. An exception is the Pt–H bond length which is strongly overestimated. Note that the Pt–H bond lengths in the square planar Pt(II) hydrides whose structures are deposited in the Cambridge Structural Database [51] vary from 1.985 Å [52] to 1.456 Å [53]. Positions of hydride protons on heavy transition metals are hardly assessed by X-ray diffraction analysis. Assuming that the $R(Pt^1–H^1)$ distance reported in [44] involves large errors, we do not place strong emphasis to the above discrepancy. The PES of complex **XX** contains no local minimum for a structure having proton on O^1. As this proton is transferred from O^2 to O^1, the energy steadily increases by 1 kcal mol^{-1}.

As the P^2H_2OH group is rotated about the $Pt–P^2$ bond, which breaks the hydrogen bond, a local minimum is attained, whose energy is 13.1 kcal mol^{-1} higher that the formation energy of complex **XX**. Such a high strength of the hydrogen bond in **XX** imparts rigidity to the ligand, which is responsible for its unique chelating properties.

We explored several alternative paths of ethylene hydroformylation on catalyst **XX**. The optimal path involves initial addition of ethylene to **XX.** This reaction fairly readily occurs as an entropy-controlled reaction (ΔH_{298} = –5.15 kcal mol^{-1}, ΔS_{298} = –41.58 e.u., ΔG_{298} = 7.25 kcal mol^{-1}) to form complex **XXI** in which ethylene is bound to platinum by the h^2 type [Eq. (10)]. It is quite notable that the coordination of ethylene makes the hydrogen atom in the $P^2–O^2–H\cdots O^1–P^1$ chain to displace to O^1.

$$\underset{\textbf{XX}}{\{[(H_2PO)_2H]Pt(PH_3)(H)]\}} + CH_2{=}CH_2 \longrightarrow \underset{\textbf{XXI}}{\{[(H_2PO)_2H]Pt(PH_3)(H)\eta^2(CH_2{=}CH_2)]\}}. \quad (10)$$

The rearrangement of **XXI** into η^1-ethyl complex **XXIII** [Eq. (11)] occurs through transition state **XXII** with the activation energy 14.15 kcal mol^{-1}.

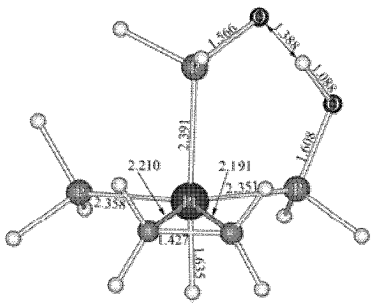

XXI

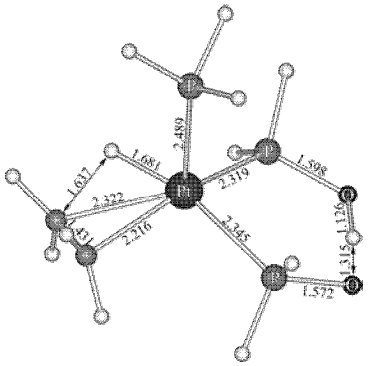

XXII

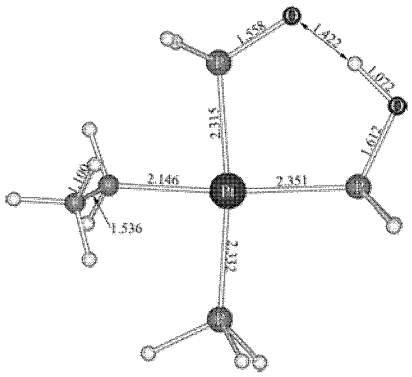

XXIII

$$\{[(H_2PO)_2H]Pt(PH_3)(H)\eta^2(CH_2{=}CH_2)]\}$$
XX

$$\longrightarrow \{[(H_2PO)_2H]Pt(PH_3)CH_2CH_3]\}. \quad (11)$$
XXIII

The process is exothermic (ΔH_{298} = –12.26 kcal mol^{-1}, ΔG_{298} = –13.89 kcal mol^{-1}). The insetion of ethylene into the Pt–H bond is accompanied by back proton transfer through the hydrogen-bond chain from O^1 to O^2.

The addition of CO to **XXIII** [Eq. (12)] is a barrierless reaction (ΔH_{298} = –10.18 kcal mol^{-1}, ΔG_{298} = –0.41 kcal mol^{-1}) yielding complex **XXIV**. This process, again, is accompanied by proton transfer over the hydrogen-bond chain.

$$\{[(H_2PO)_2H]Pt(PH_3)CH_2CH_3]\} + CO$$
XXIII

$$\longrightarrow \{[(H_2PO)_2H]Pt(PH_3)(CO)CH_2CH_3]\}. \quad (12)$$
XXIV

Exothermic isomerization (ΔH_{298} = –8.98 kcal mol^{-1}, ΔG_{298} = –8.86 kcal mol^{-1}) of complex **XXIV** into a square-planar η^1-acyl complex **XXVI** [Eq. (13)] then occurs, which is associated with overcoming the highest energy barrier in this reaction path, corresponding transition state **XXV** (activation energy ΔE_a^0 = 17.60 kcal mol^{-1}). This process also involves proton transfer over the hydrogen-bond chain.

$$\{[(H_2PO)_2H]Pt(PH_3)(CO)CH_2CH_3]\}$$
XXIV

$$\longrightarrow \{[(H_2PO)_2H]Pt(PH_3)COCH_2CH_3]\}. \quad (13)$$
XXVI

Oxidative addition of a hydrogen molecule to **XXVI** [Eq. (14)] gives rise to an octahedral *cis*-dihydride **XXVIII**. This is an entropy-controlled process (ΔH_{298} = –2.01 kcal mol^{-1}, ΔG_{298} = 9.69 kcal mol^{-1}, ΔE_a^0 = 12.41 kcal mol^{-1}) that passes through transition state **XXVII**.

The final stage of the catalytic cycle is an exothermic (ΔH_{298} = –0.86 kcal mol^{-1}, ΔG_{298} = –14.25 kcal mol^{-1}) reductive elimination of propanal [Eq. (15)]; it passes through transition state **XXVII** with the activation energy ΔE_a^0 15.51 kcal mol^{-1}.

$$\{[(H_2PO)_2H]Pt(PH_3)(H)_2COCH_2CH_3]\} + H_2$$
XXVI

$$\longrightarrow \{[(H_2PO)_2H]Pt(H)_2(PH_3)COCH_2CH_3]\}, \quad (14)$$
XXVII

$$\{[(H_2PO)_2H]Pt(H)_2(PH_3)COCH_2CH_3]\}$$
XXVIII

$$\longrightarrow \{[(H_2PO)_2H]Pt(H)(PH_3)]\} + C_2H_5CHO. \quad (15)$$
XX

Detailed study of the PES and possible alternative paths of the catalytic process shows that the above-described catalytic cycle (Fig. 4) is optimal in terms of both kinetics and thermodynamics. This conclusion agrees with the experimental findings of Van Leeuwen [43].

As known, the hydroformylation of alkenes is accompanied by their hydrogenation as the side process. The latter process can involve oxidative addition of hydrogen to **XXIII** followed by elimination of ethane:

$$\{[(H_2PO)_2H]Pt(PH_3)CH_2CH_3]\} + H_2$$
XXIII

$$\longrightarrow \{[(H_2PO)_2H]Pt(PH_3)(H)_2CH_2CH_3, \quad (16)$$
XXIX

$$\{[(H_2PO)_2H]Pt(PH_3)(H)_2CH_2CH_3$$

$$\longrightarrow \{[(H_2PO)_2H]Pt(PH_3)H]\} + C_2H_6. \quad (17)$$

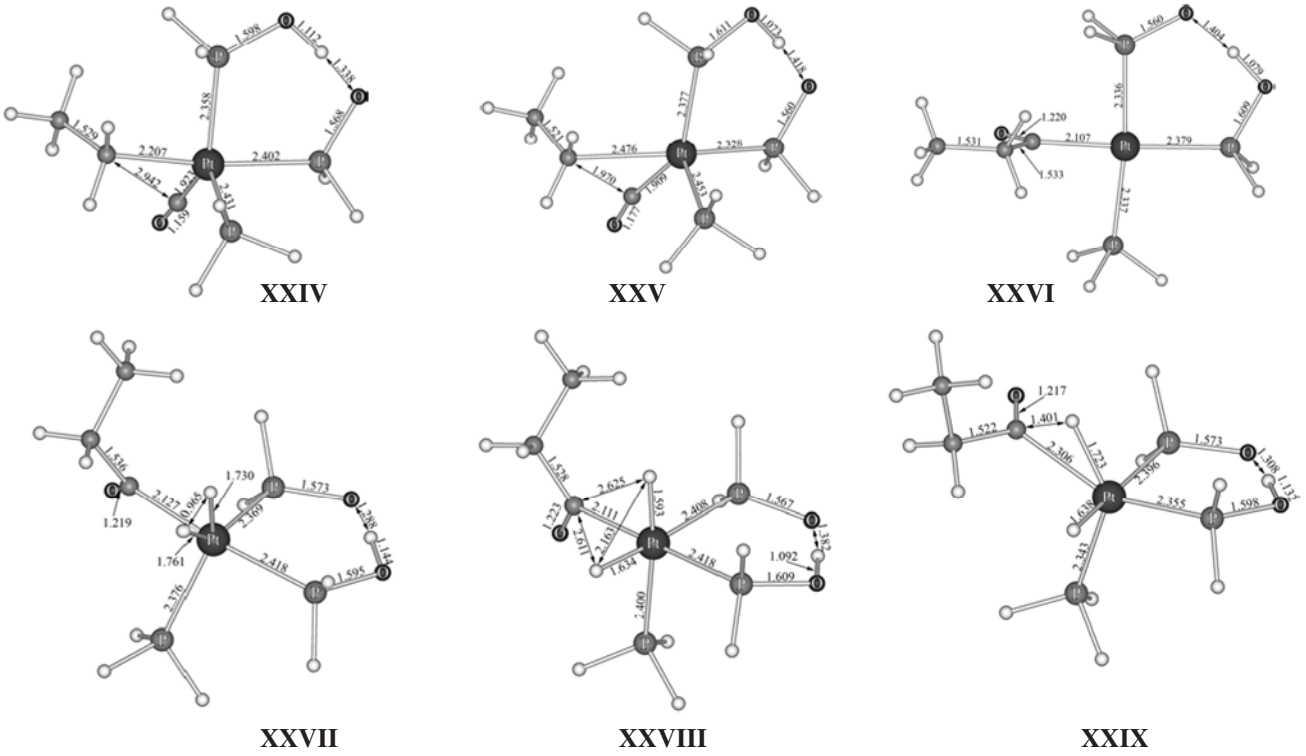

XXIV **XXV** **XXVI**

XXVII **XXVIII** **XXIX**

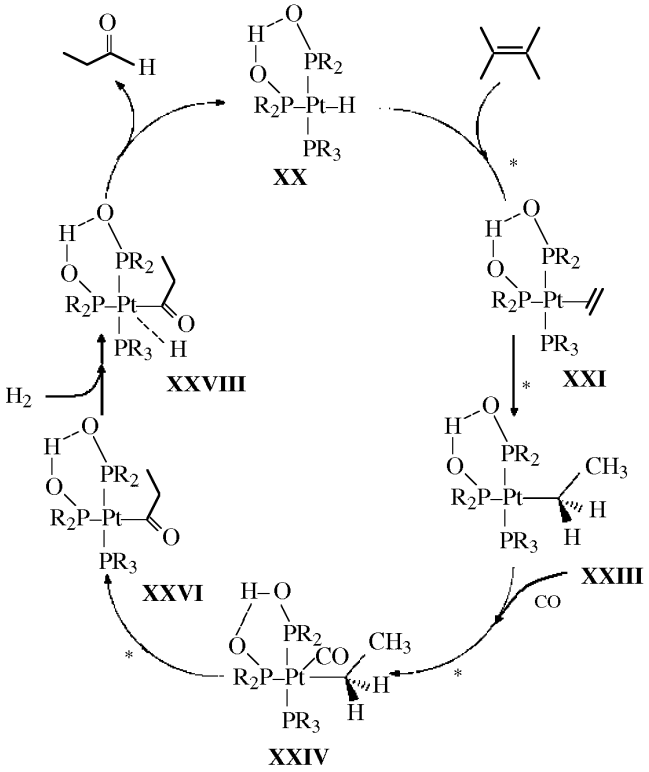

Fig. 4. Scheme of the catalytic cycle of ethylene hydroformylation on complex **XX**. Starred are stages involving proton migration over the P–O–H···O=P chain.

The calculations show that the activation energy of H_2 addition to **XXIII** is 14.15 kcal mol^{-1}, and the final reaction product is dihydride **XXIX**. The process is entropy-controlled and endothermic (ΔH_{298} = 1.44 kcal mol^{-1}, ΔS_{298} = –32.55 e.u., ΔG_{298} = 11.14 kcal mol^{-1}).

The subsequent elimination of ethane from 29 is a strongly exothermic reaction with the activation energy 13.93 kcal mol^{-1} (ΔH_{298} = –18.61 kcal mol^{-1}, ΔG_{298} = –30.25 kcal mol^{-1}).

Since the addition of CO to **XXIII** is a barrierless and an exothermic reaction [Eq. (12)], whereas for molecular hydrogen to add to **XXIII** [Eq. (16)] requires overcoming an appreciable energy barrier (14.15 kcal mol^{-1}) and is endothermic, the contribution of hydrogenation as a competing process in mild conditions should not be considerable, provided the reaction medium does not contain excess hydrogen. Evidence for this conclusion comes from the experimental data of Van Leeuwen.

CONCLUSION

The theoretical simulation shows that the high efficiency of complexes like **XVI** and **XX** as catalysts of homogeneous hydroformylation of alkenes is explained by the following reasons.

1. The presence of a free coordination site in these square-planar platinum complexes makes possible coordination of alkene at the first stage without the energetically unfavorable preliminary dissociation of one of the metal–ligand bonds.

2. The high strength of the hydrogen bon in P–O–H· · ·O=P complexes favors formation in the coordination sphere of the metal of a bidentate ligand which fairly rigidly fixes the geometry of the catalytic center, which, as known, enhances the regioselectivity of the hydroformylation reaction.

3. The proton in the P–O–H···O=P chain readily migrates along this chain and thus provides fine tuning of the electron density in the catalytic cycle at each reaction step.

We place particular emphasis on the latter observation. A great number of enzymatic processes are known, in which proton transfer plays the role of molecular trigger for the entire multistage process. In our case, proton migration functions as molecular switcher. We are the first to observe this phenomenon in reactions catalyzed by metal complexes.

The presented results of the theoretical research of the structure and reactivity of hydrophosphoryl compounds and the mechanisms of hydroformylation and hydrogenation reactions on their platinum complexes allow the established regularities to be used in the design of novel catalytic systems. We are presently actively working in this direction.

ACKNOWLEDGMENTS

The authors are grateful to the Russian Foundation for Basic Research for financial support of this research (project no. 08-03-00586).

REFERENCES

1. Davidsonб E.R., *Chem. Rev*., 2000, vol. 100, p. 351.
2. Ziegler, T., *Chem. Rev*., 1991, vol. 91, p. 651.
3. Gambarotta, S., Arena, F., Floriani, C., and Zanazzi, P.F., *J. Am. Chem. Socю*, 1982, vol. 104, p. 5082.
4. Lemke, F.R. and Bullock, R.M., *Organometallics*, 1992, vol. 11, p. 4261.
5. Pinkes, J.R., Steffey, B.D., Vites, J.C., and Cutler, A.R., *Ibid*., 1994, vol. 13, p. 21.
6. Hanna, T.A., Baranger, A.M., and Bergman, R.G., *J. Am. Chem. Soc.*, 1995, vol. 117, p. 11363.
7. Rerdew, J.P., Burke, K., and Ernzerhof, M., *Phys. Rev. Lett*., 1996, vol. 77, p. 3865.
8. Laikov, D.N., *Chem. Phys. Lett*., 1997, vol. 281, p. 151.
9. Laikov, D.N. and Ustynyuk, Yu.A., *Izv. Akad. Nauk, Ser. Khim.*, 2005, no. 3, p. 804.
10. Stevens, W.J., Basch, H., and Krauss, M., *J, Chem. Phys*., 1984, vol. 81, p. 6026.
11. Stevens W.J., Krauss M., Basch H., and Jasien P.G., *Can. J. Chem.*, 1992, p. 612.
12. Cundari T.R. and Stevens W.J., *J. Chem. Phys*., 1993, vol. 98, p. 5555.
13. *http://www.cmbi.ru.nl/molden/molden.html.*
14. Hirshfeld, F.L., *Theor. Chim. Acta. (Berl.)*, 1977, vol. 44, p. 129.
15. Nifant'ev, E.E., *Khimiya gidrofosforil'nykh soedinenii* (Chemistry of Hydrophosphoryl Compounds), Moscow: Nauka, 1983.
16. Stawinski, J. and Kraszewski, A., *Acc. Chem. Res.,* 2002, vol. 35, p. 952.
17. Hoge, B., Neufeind, S., Hettel, S., Wiebe, W., and Thosen, C., *J. Organomet. Chem.*, 2005, vol. 690, p. 2382.
18. Hoge, B., Garcia, P., Willner, H., and Oberhammer, H., *Chem. Eur. J*., 2006, vol. 12, p. 3567.
19. Nifant'ev, E.E., Zavalishina, A.I., Sorokina, S.F., and Borisenko, A.A., *Zh. Obshch. Khim*., 1976, vol. 46, p. 471.
20. Ovchinnikov, V.V., Cherezov, S.V., Cherkasov, R.A., and Pudovik, A.N., *Ibid*., 1984, vol. 54, no. 5, p. 1021.
21. Mamaev, V.M., Prisyajnuk, A.V., Babin, Y.V., Logutenko, L.S., and Laikov, D.N., *Mendeleev Commun.*, 1999, no. 6, p. 240.
22. Babin, Yu.V., Kalinov, S.M., and Prisyazhnyuk, A.V., *Zh. Strukt. Khim*., 2003, vol. 44, no. 5, p. 944.
23. Wesolowski, S.S., Brinkmann, N.R., Valeev, E.F., Shaefer III, H.F., et al., *J. Chem. Phys*., 2002, vol. 116, p. 112.
24. Sola, M. and Toro-Labbé, A., *J. Phys. Chem. A*, 1999, vol. 103, p. 8847.
25. Babin, Yu.V., Prisyazhnyuk, A.V., and Ustynyuk, Yu.A., *Zh. Fiz. Khim.*, 2008, vol. 82, no. 1, p. 1.
26. Steiner, T., *Angew. Chem. Int. Ed*., 2002, vol. 41, p. 48.
27. Desiraju, G.R., *Acc. Chem. Res.*, 1996, vol. 29, p. 441.
28. Steiner, T., Maas, J., and Lutz, B., *J. Chem. Soc. Perkin Trans. 2*, 1997, p. 1287.
29. Steiner, T. and Desiraju, G.R., *Chem. Commun*., 1998, p. 891.
30. Steiner, T., *New J. Chem*., 1998, p. 1099.
31. Gu, Y., Kar, T., and Scheiner, S., *J. Am. Chem. Soc.,* 1999, vol. 121, p. 9411.
32. Bader, R.F.W., *Atoms in Molecules: A Quantum Theory,* Oxford, U.K.: Oxford Univ. Press, 1990.
33. Prisyazhnyuk, A.V. and Babin, Yu.V., *Zh. Strukt. Khim.*, 2005, vol. 46, no. 1, p. 166.

34. Chatt, J. and Heaton, B.T., *J. Chem. Soc. A*, 1968, p. 2745.
35. Li, G.Y., *J. Organomet. Chem.*, 2002, vol. 653, p. 63.
36. Walther, B., *Coord. Chem. Rev.*, 1984, vol. 60, p. 67.
37. Appleby, T. and Woollins, J.D., *Ibid.*, 2002, vol. 235, p. 121.
38. Khanapure, S.P. and Garvey, D.S., *Tetrahedron Lett.*, 2004, vol. 45, p. 5283.
39. Wolf, C. and Lerebours, R., *J. Org. Chem.*, 2003, 68, no. 18, p. 7077.
40. Wolf, C. and Lerebours, R., *Org. Biomol. Chem.*, 2004, no. 2, p. 2161.
41. Li, G.Y., *J. Org. Chem.*, 2002, vol. 67, no. 11, p. 3643.
42. *http://www.combiphos.com/.*
43. Van Leeuwen, P.W.N.M., Roobeek, C.F., Wife, R.L., and Frijns, J.H.G., *J. Chem. Soc., Chem. Commun.*, 1986, p. 31.
44. Han, L.-B., Choi N., and Tanaka, M., *Organometallics,* 1996, vol. 15, p. 3259.
45. Dubrovina, N.V. and Borner, A., *Angew. Chem. Int. Ed.*, 2004, vol. 43, p. 5883, and references therein.
46. Breit, B. and Seiche, W., *J. Am. Chem. Soc.*, 2003, vol. 125, p. 6608.
47. Musaev, D.G. and Morokuma, K., *Adv. Chem. Phys.,* 1996, vol. 95, p. 61.
48. Ziegler, T., Cavallo, L., and Berces, A., *Organometallics*, 1993, vol. 12, p. 3586.
49. Alagona, G., Ghio, C., Lazzaroni, R., and Settambolo, R., *Ibid.*, 2001, vol. 20, p. 5394.
50. Decker, S.A. and Gundari, T.R., *Ibid.*, 2001, vol. 20, p. 2827.
51. *http://www.ccdc.cam.ac.uk.*
52. Furalani, A., Licoccia, S., Russo, M.V., et al., *J. Chem. Soc., Dalton Trans.*, 1982, p. 2449.
53. Ara, I., Berenguer, J.R., Eguizabal, E., et al., *Organometallics*, 2000, vol. 19, p. 4385.